

## Strength assessment of Al-Humic and Al-Kaolin aggregates by intrusive and non-intrusive methods

Moruzzi, Rodrigo; da Silva, Pedro Grava; Sharifi, Soroosh; Campos, Luiza C.; Gregory, John

DOI:

[10.1016/j.seppur.2019.02.033](https://doi.org/10.1016/j.seppur.2019.02.033)

License:

Creative Commons: Attribution-NonCommercial-NoDerivs (CC BY-NC-ND)

*Document Version*

Peer reviewed version

*Citation for published version (Harvard):*

Moruzzi, R, da Silva, PG, Sharifi, S, Campos, LC & Gregory, J 2019, 'Strength assessment of Al-Humic and Al-Kaolin aggregates by intrusive and non-intrusive methods', *Separation and Purification Technology*, vol. 217, pp. 265-273. <https://doi.org/10.1016/j.seppur.2019.02.033>

[Link to publication on Research at Birmingham portal](#)

**Publisher Rights Statement:**

Checked for eligibility: 20/03/2019

**General rights**

Unless a licence is specified above, all rights (including copyright and moral rights) in this document are retained by the authors and/or the copyright holders. The express permission of the copyright holder must be obtained for any use of this material other than for purposes permitted by law.

- Users may freely distribute the URL that is used to identify this publication.
- Users may download and/or print one copy of the publication from the University of Birmingham research portal for the purpose of private study or non-commercial research.
- User may use extracts from the document in line with the concept of 'fair dealing' under the Copyright, Designs and Patents Act 1988 (?)
- Users may not further distribute the material nor use it for the purposes of commercial gain.

Where a licence is displayed above, please note the terms and conditions of the licence govern your use of this document.

When citing, please reference the published version.

**Take down policy**

While the University of Birmingham exercises care and attention in making items available there are rare occasions when an item has been uploaded in error or has been deemed to be commercially or otherwise sensitive.

If you believe that this is the case for this document, please contact [UBIRA@lists.bham.ac.uk](mailto:UBIRA@lists.bham.ac.uk) providing details and we will remove access to the work immediately and investigate.

1                   **STRENGTH ASSESMENT OF AL-HUMIC AND AL-KAOLIN**  
2                   **AGGREGATES BY INTRUSIVE AND NON-INTRUSIVE METHODS**

3  
4  
5 Rodrigo B. Moruzzi<sup>a\*</sup>, Pedro Grava da Silva<sup>b</sup>, Soroosh Sharifi<sup>c</sup>, Luiza C. Campos<sup>d</sup>, John  
6 Gregory<sup>d</sup>

7  
8  
9  
10 <sup>a</sup> Instituto de Geociências e Ciências Exatas, Univ. Estadual Paulista (UNESP), Av. 24-A, 1515,  
11 Jardim Bela Vista, Rio Claro, 13506-900. São Paulo, Brazil. E-mail: [rmoruzzi@rc.unesp.br](mailto:rmoruzzi@rc.unesp.br)

12 <sup>b</sup> Programa de Pós-graduação em Engenharia Civil e Ambiental, Univ. Estadual Paulista  
13 (UNESP), Av. 24-A, 1515, Jardim Bela Vista, Rio Claro, 13506-900. São Paulo, Brazil. E-mail:  
14 [pedroagrava@gmail.com](mailto:pedroagrava@gmail.com)

15 <sup>c</sup> Department of Civil Engineering, University of Birmingham, B15 2TT, United Kingdom.  
16 Email: [S.Sharifi@bham.ac.uk](mailto:S.Sharifi@bham.ac.uk)

17 <sup>d</sup> Department of Civil, Environmental and Geomatic Engineering, University College London,  
18 Gower St, London, WC1E 6BT, United Kingdom. E-mail: [l.campos@ucl.ac.uk](mailto:l.campos@ucl.ac.uk)

19  
20  
21  
22  
23  
24  
25  
26  
27  
28  
29  
30 **Address:**

31 \* Corresponding author: Avenida 24-A, nº 1515, C. P. 178, CEP 13506-900, Office 23, Bela Vista, Rio  
32 Claro, São Paulo, Brazil. Phone: +55 19 3526-9339. E-mail address: [rmoruzzi@rc.unesp.br](mailto:rmoruzzi@rc.unesp.br)

33 **Abstract:**

34 Resistance to breakage is a critical property of aggregates generated in water and wastewater  
35 treatment processes. After flocculation, aggregates should ideally keep their physical  
36 characteristics (i.e. size and morphology), to result in the best performance possible by individual  
37 separation processes. The integrity of aggregates after flocculation depends upon their capacity to  
38 resist shear forces while transported through canals, passages, apertures, orifices and other  
39 hydraulic units. In this study, the strength of Al-Humic and Al-Kaolin aggregates was  
40 investigated using two macroscopic measurement techniques, based on both intrusive and non-  
41 intrusive methods, using image analysis and light scattering based equipment. Each technique  
42 generates different information which was used for obtaining three floc strength indicators,  
43 namely, strength factor ( $SF$ ), local stress from the hydrodynamic disturbance ( $\sigma$ ) and the force  
44 coefficient ( $\gamma$ ) for two different study waters. The results showed an increasing trend for the  $SF$  of  
45 both Al-Humic and Al-Kaolin aggregates, ranging from 29.7% to 78.6% and from 33.3% to  
46 85.2%, respectively, in response to the increase of applied shear forces during flocculation (from  
47 20 to 120  $s^{-1}$ ). This indicates that aggregates formed at higher shear rates are more resistant to  
48 breakage than those formed at lower rates. In these conditions,  $\sigma$  values were observed to range  
49 from 0.07 to 0.44  $N/m^2$  and from 0.08 to 0.47  $N/m^2$  for Al-Humic and Al-Kaolin, respectively.  
50 Additionally, it was found that for all studied conditions, the resistance of aggregates to shear  
51 forces was nearly the same for Al-Humic and Al-Kaolin aggregates, formed from destabilized  
52 particles using sweep coagulation. These results suggest that aggregate strength may be mainly  
53 controlled by the coagulant, emphasizing the importance of the coagulant selection in water  
54 treatment. In addition, the use of both intrusive and non-intrusive techniques helped to confirm  
55 and expand previous experiments recently reported in literature.

56

57 **Keywords:** Aggregates, floc resistance, image analysis, flocculation.

## 58        **1. Introduction**

59        Most solid-liquid separation processes work by increasing the size of the particulate matter,  
60        leading to the formation of aggregates or flocs. The performance of solids removal is dependent  
61        on the physical characteristics of the aggregates that need to be compatible with the separation  
62        method used (Yukselen and Gregory, 2004). Among these characteristics, the floc strength,  
63        which is an expression of resistance to breakage, is crucial for effective particle separation in  
64        clarification units, such as sedimentation tanks, dissolved air flotation units and membrane  
65        filtration (Jarvis *et al.*,2005).

66        It is well-documented that, solid-liquid processes are negatively affected by the breakage of flocs,  
67        as only limited regrowth of broken flocs can occur, thus leading to low removal efficiency in  
68        sedimentation units (Yukselen and Gregory, 2002, 2004; Yu *et al.*, 2010b, 2011, 2015). The floc  
69        strength is also linked to problems in treatment plants with rapid sand filtration, in which the  
70        small resistance of the aggregates to the hydrodynamic variations has a damaging impact on the  
71        filter media, shortening their operational life and resulting in pollutant trespassing (Moruzzi and  
72        Silva, 2018). Therefore, water treatment plants should ideally be designed to minimize floc  
73        breakage; however, despite the recommendations, it is difficult to precisely determine how much  
74        stress a previously formed floc can take without breaking.

75        When the shear rate is larger than floc strength, the flocs either break into approximately equal  
76        size fragments, or under some circumstances, erosion of small particles from the flocs' surface  
77        may occur. In turbulent flow, the breakage type depends on the size of the flocs in relation to the  
78        micro-scale of turbulence (Mühle, 1993). Because of floc breakage, some regions of the floc  
79        surface may become inactive and incapable of forming new bonds of attachment to other flocs,  
80        thus reducing the flocculation efficiency (Yu *et al.*, 2011). The fact that broken flocs do not fully  
81        regrow when the original low shear rate is restored means that the binding between particles is  
82        weaker (Yu *et al.*, 2010b).

83        It is well acknowledged that the floc strength is dependent on the bonds between aggregate  
84        component particles (Parker *et al.*, 1972, Bache *et al.*, 1997). This includes the strength and  
85        number of individual bonds within the floc. However, recent studies (e.g. Yu *et al.*, 2015) have  
86        shown that kaolin particles incorporated within hydroxide flocs appear to have no influence on  
87        floc properties, including floc strength and size. Younker and Walsh (2016) demonstrated that the

88 addition of adsorbents to metallic salt flocs did not increase or reduce floc strength. Conversely,  
89 kaolin flocs formed by ferric coagulants were found to be larger and stronger than those formed  
90 by alum coagulants (Zhong *et al.*, 2011). Bridging flocculation by long-chain polymers can  
91 generate very resistant flocs, while the destabilization of particles by low dosages of inorganic  
92 salts results in fairly weak flocs (Yukselen and Gregory, 2004; Wang *et al.*, 2009; Yu *et al.*,  
93 2015).

94 Humic acids have been widely used as natural organic matter to investigate floc properties after  
95 flocculation. It has been shown that humic flocs growth is not determined by the flocs' size  
96 distribution (Yu *et al.*, 2010b, 2012), but by some of their properties, including floc strength,  
97 which is mostly dependent on the surface activity of flocs, and coagulant species formed from  
98 Alum and Iron hydrolysis (Wang *et al.*, 2009).

99 Moruzzi and Silva (2018) carried out experiments on Al-Humic and Al-Kaolin aggregates and  
100 showed that flocs formed from sweep coagulation mechanism, by different particulate matter and  
101 the same coagulant have similar regrowth patterns, indicating similar binding between particles  
102 for Al-Humic and Al-Kaolin, as presented by Yu *et al.* (2010b). On the basis of these findings, it  
103 is speculated that Al-Humic flocs strength might have similar resistance to shear forces as Al-  
104 Kaolin flocs. In this case, the resistance of the flocs to shear rate could be attributed to the used  
105 coagulant, corroborating with results presented by Yu *et al.* (2015).

106 For determining aggregate proprieties, such as size and floc strength, monitoring techniques  
107 should be applied during flocculation. Intrusive techniques, such as those based on light  
108 scattering, have been conventionally used for monitoring aggregates during flocculation  
109 (Yukselen and Gregory, 2002; 2004; Yu *et al.*, 2011). However, these techniques require taking  
110 frequent samples from the water into measurements chambers, a process that may cause some  
111 damage to aggregates due to their fragile nature. In some cases, flocs damage may be minimized  
112 by limiting the average gradient velocity during the sample extraction, controlling inner tube size  
113 and flow through tube, as presented by Gregory (1981) and Yu *et al.* (2010b). Recently,  
114 however, flocculation monitoring by non-intrusive image analysis has shown promising results  
115 (Li *et al.*, 2007; Moruzzi *et al.*, 2017; Moruzzi and Silva, 2018) and has allowed the  
116 determination of floc strength, among other floc characteristics.

117 In practice, the strength of the floc is often determined in an empirical way, usually by  
118 establishing a relationship between the floc size and the applied shear rate (François, 1987; Jarvis  
119 *et al.*, 2005, Li *et al.*, 2007). This empirical approach was firstly suggested by Parker *et al.*  
120 (1972), and it has been used extensively in theoretical and experimental research to evaluate  
121 maximum floc size under a given turbulent intensity (e.g. Bache, 1989; 2004 and Li *et al.*, 2006;  
122 2007).

123 There are two fundamental approaches to measuring the strength of the floc *i.e.* a macroscopic  
124 approach, which measures the system energy required for breakage of flocs, and a microscopic  
125 approach, which measures the interparticle forces within individual flocs (Jarvis *et al.*, 2005). In  
126 the microscopic approach, the strength can be measured by applying a shear stress or a normal  
127 stress to a floc individually. On the other hand, macroscopic techniques perform an indirect  
128 evaluation of the floc resistance by means of analysing the energy dissipation, or the mean  
129 velocity gradient ( $G$ ), applied to maximum- or average-sized flocs. This approach originated from  
130 the empirical relationship between the applied hydrodynamic shear rate and the resulted floc size  
131 (Jarvis *et al.*, 2005).

132 This work aims to investigate the floc strength for both Al-Kaolin and Al-Humic aggregates by  
133 means of macroscopic indicators, and to demonstrate the insignificant effect of the particulate  
134 matter within the flocs on their properties, namely size and strength. For the first time, image  
135 analysis is applied concomitantly with photometric dispersion to obtain the strength factor ( $SF$ ),  
136 local stress from the hydrodynamic disturbance ( $\sigma$ ) and the force coefficient ( $\gamma$ ). The combined  
137 application permits the comparison and establishment of correlations between the data obtained  
138 from two different techniques (intrusive and non-intrusive). This is the first time image and  
139 photometric dispersion of Al-Humic acid flocs is measured by this technique and the results from  
140 the two complementary methods is used to understand the factors affecting floc strength.

## 141 **2. Materials and Methods**

### 142 *2.1 Study Waters*

143 Two water samples were prepared from stock suspension of kaolin and from stock solution of  
144 humic acid. For sample one, hereafter referred to as type 1, a humic acid solution prepared from  
145 lyophilised natural organic matter (*Aldrich Chemical*) with concentration of 30 mg/L was used to  
146 obtain 50 units of Platinum-Cobalt Scale - PtCo at 455 nm, as the initial condition (Moruzzi and

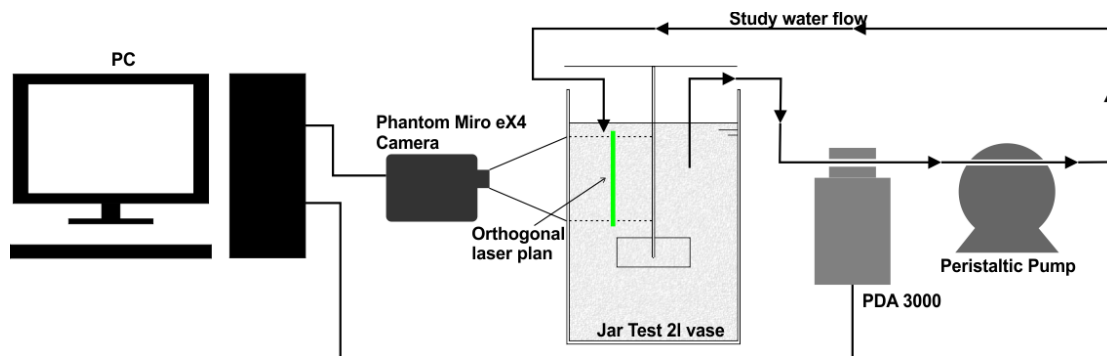
147 Silva, 2018). For the second sample (type 2), a kaolin suspension was prepared from a  
148 commercial kaolin (Sigma-Aldrich) to obtain 25 units of turbidity scale as Nephelometric  
149 Turbidity Units - NTU (Moruzzi *et. al*, 2017 and Yukselen and Gregory, 2004).

150 Coagulation was performed by dosing alum  $[\text{Al}_2(\text{SO}_4)_3 \cdot 18\text{H}_2\text{O}]$  using sweep-coagulation  
151 mechanism, following recommendations by Oliveira *et al.* (2015). So, dosages of 10 and 30  
152  $\text{mgAl}^{+3}/\text{l}$  at pH of 7.5 and 4.5 were applied for Al-Kaolin and Al-Humic aggregates formation,  
153 respectively. Sodium hydroxide (NaOH) 1 mM was used as a buffer during coagulation to control  
154 pH. All tests were performed at room temperature ( $20 \pm 2$  °C).

### 155 *2.2 Flocculation and strength tests*

156 Jar tests were performed for flocculation and breakage experiments (*Ethik Technology Model*  
157 *218/6 LDB*). The method applied consists of an intrusive and non-intrusive image-based  
158 acquisition method and photometric dispersion analyser (PDA), similar to that used by Yu *et al.*  
159 (2015). Here, however, both image and photometric dispersion were applied at the same time to  
160 obtain strength indices, thus permitting comparison and correlation of results. A simplified  
161 schematic of the experimental apparatus, including Jar Test, the image-based system and light-  
162 scattering monitoring equipment, is shown in Figure 1.

163 A mean velocity gradient of  $800 \text{ s}^{-1}$  was applied for 10 seconds to ensure a rapid mixing, and also  
164 for flocs breakage in all light scattering tests, based on preliminary tests (Oliveira *et al.*, 2015).  
165 This standard shear rate was chosen for taking a central position in the typical shear range of  
166 predominant erosion breakage as proposed by Mikkelsen and Keiding (2002), and the duration  
167 was sufficient for the coagulant transportation (Yukselen and Gregory, 2004). For flocculation,  
168 the following velocity gradients ( $G$ ) were applied: 20, 30, 40, 50, 60, 80, 100 and  $120 \text{ s}^{-1}$ . For the  
169 trials involving PDA measurements,  $G$  values were kept constant during the first 25 minutes, and  
170 after this period,  $G$  was set to  $800 \text{ s}^{-1}$  for 10 seconds to induce breakage of flocs. This short period  
171 of time was chosen to simulate the water passage in gates and orifices that normally occur after  
172 flocculation.



173

174 Figure 1. A simplified schematic of the experimental apparatus.

175

### 176 2.3 Image Analysis

177 The image analysis applied here was strictly used to obtain aggregates size, which in turn was  
 178 used for floc strength indicator calculations, namely local stress from the hydrodynamic  
 179 disturbance ( $\sigma$ ) and the force coefficient ( $\gamma$ ), as presented in Section 2.6. Images were captured in  
 180  $2^8$  bit monochromatic mode (*i.e.* 256 grey scale) using a *Vision Research Miro EX4* camera  
 181 together with a set of lenses, and 840 pixel x 640 pixel of image resolution, to obtain a pixel size  
 182 of 10  $\mu\text{m}$ . A laser sheet of 20,000 mW and wavelength of 520 nm provided the lighting as  
 183 described by Oliveira *et al.* (2015) and Moruzzi *et al.* (2017).

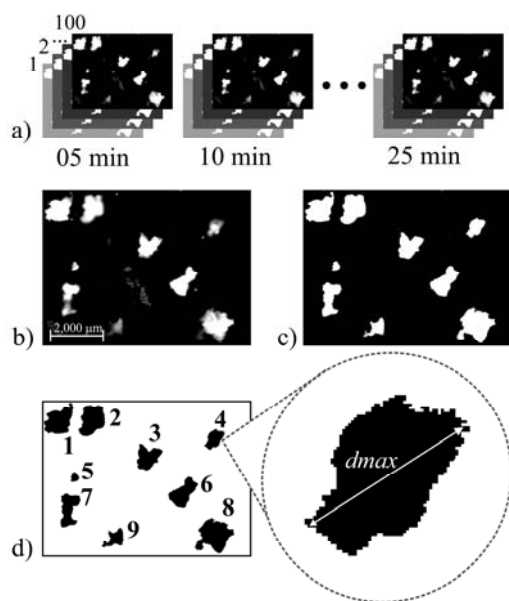
184 Samples were obtained at 5-minute intervals (from 5 to 25 minutes) to assess floc size at a given  
 185 flocculation time ( $T$ ) of interest, *i.e.* those usually applied in drinking water treatment plants.  
 186 Each image package was taken over a short duration of 10 seconds with a frequency of 10 Hz  
 187 (Figure 2-a) to precisely describe the system situation at that given time of interest. This sample  
 188 time and frequency was sufficient to capture a reliable picture of the floc characteristics at the  
 189 required flocculation time along with a statically representative number of flocs within the 10  
 190 seconds sampling time.

191 The image processing software *Image-Pro-Plus*® (IPP) was used to develop the images, *i.e.*  
 192 conversion from  $2^8$  to  $2^1$  bits, enhancement and measurement (Figures 2-b to 2-d). Only  
 193 aggregate sizes longer than 100  $\mu\text{m}$  ( $\geq 10$  pixels) were monitored for image precision, as  
 194 recommended by Chakraborti *et al.* (2003).

195 In total, 197,207 aggregates were measured from 7,200 frames (average of 27 aggregates/frame)  
 196 for Al-Humic water, and 141,609 aggregates were measured from 6,800 frames (average of 21



197 aggregates/frame) for Al-Kaolin water. In these sample sizes, floc size errors were lower than  
 198 4.0% and 4.6% at 95% of confidence interval for an infinite population of Al-Humic and Al-  
 199 Kaolin aggregates, respectively. Figure 2 illustrates the different steps involved in the image  
 200 processing procedure applied here, from acquisition to image processing and size measurement.



201

202 Figure 2. An example of image conversion enhancement and measurement: (a) Image acquisition  
 203 using on 10 Hz during 10 seconds for each flocculation time (T), resulting in a pack of 100 frames  
 204 per  $G \times T$ ; (b) Floccs in grey scale ( $2^8$  bits); (c) Image after threshold with black and white pixels  
 205 only ( $2^1$  bits); (d) Counting and measuring floccs by IPP 7.0 software®.

#### 206 2.4 Light Scattering

207 The light scattering approach applied was strictly used to obtain the flocculation index (FI),  
 208 which will be better explained in the following sections. Light scattering analysis was performed  
 209 using a *Photometric Dispersion Analyser* (PDA), and the obtained results were used for  
 210 calculating the strength factor, which will be introduced and presented in Section 2.6. In PDA  
 211 equipment, samples flow through a 3-mm-diameter tube where the intensity of a narrow beam of  
 212 light is monitored by a sensitive photodetector following Yukselen and Gregory (2004) and  
 213 Moruzzi *et al.* (2017). Although intrusive technologies can cause some damage to floccs, in PDA  
 214 this can be minimised by controlling the average gradient velocity during sample extraction.  
 215 Here, the flow rate through the sampling tube was controlled to enforce laminar flow regime

216 (Reynolds number  $\leq 80$ ) and shear rates lower than  $50 \text{ s}^{-1}$ , as shown by Gregory (1981);  
217 conditions where damage is considered insignificant, as also shown by Yu *et al.*, 2010b. Further,  
218 the water samples were circulated by means of a peristaltic pump located after the PDA  
219 instrument to avoid the effects of possible floc breakage in the pinch part of the pump (Figure 1),  
220 as performed by Li *et al.* (2007).

221 The *PDA 3000* measures the average transmitted light intensity (dc value) and the root mean  
222 square (rms) value of the fluctuating component. The ratio (rms/dc) provides a measure of the  
223 balance of particle aggregation (Gregory, 1984; Gregory and Nelson, 1986; Yukselen and  
224 Gregory, 2004; Yu *et al.*, 2010b), hereafter referred to as flocculation index (*FI*). Up to a limited  
225 size, the *FI* value is strongly correlated with floc size and always increases as flocs grow larger,  
226 but the *FI* value can become uncertain when flocs are larger than  $250 \mu\text{m}$  and absolute floc size  
227 cannot be taken from *FI* signals (Yu *et al.*, 2010a; Yu *et al.*, 2010b and 2011). Also, larger  
228 aggregates have a predominant influence on the ratio value (Gregory, 1984), thus affecting *FI*  
229 signals. Therefore, the PDA shows qualitative changes in flocs, as reported by Gregory and  
230 Nelson (1986), but the instrument is unable to give an absolute particle size. Further, the *FI*  
231 signals vary with both particle size and particle number and it is not possible to know the precise  
232 contribution of each of these components in the *FI* signal. Yu *et al.* (2015) have shown that flocs  
233 with similar size can have very different *FI* values, confirming the idea that *FI* does not give an  
234 absolute indication of size for hydroxide flocs. However, the generated signal can be used as an  
235 indicator of aggregation, as shown by Gregory (1985), and also as a measure of floc strength as  
236 shown by Li *et al.* (2007), Gregory (2009) and Yu *et al.* (2010b). More details are given in the  
237 following sections.

238

### 239 2.5 Floc size and *FI* determination

240 The macroscopic techniques used for the study of the floc strength were developed based on the  
241 relationship between the applied hydrodynamic shear rate and the resulting floc size. According  
242 to Gregory (2003), floc size and *FI* can be both used as floc strength indicators for a given shear  
243 rate. In order to obtain the floc strength indicators, which are related directly to the size limit  
244 reached by the floc, two different sources of information were utilized: one from the image  
245 analysis and another from the PDA.

246 For image analysis, the average diameter ( $d$ ) of aggregates was determined from the average of  
247 the longest length of the aggregates ( $d_{max}$ ) in the selected times of interest, following Li *et al.*  
248 (2007):

$$249 \quad d = \frac{1}{n} \sum_{i=1}^n d_{imax} \quad (1)$$

250 where  $d$  is the average of  $d_{max}$  ( $\mu\text{m}$ ),  $d_{max}$  is the longest length ( $\mu\text{m}$ ), as shown in Figure 2, and  $n$   
251 is the number of counted aggregates in a sample varying from  $i = 1, 2 \dots, n$ .

252  
253 The  $d$  values obtained from Equation 1 represents the average of  $d_{max}$ , measured for each one of  
254 the eight investigated flocculation times (T), *i.e.* 5, 10, 15, 20, 25, 30, 35 or 40 minutes. It is  
255 important to emphasize that, flocculation kinetics were not the focus of this paper, but rather the  
256 floc strength assessment at given flocculation times of interest, where the dynamic equilibrium  
257 between flocs breakage and aggregation could be indirectly observed by the floc size. Therefore,  
258 the  $d$  value represents the balance between flocs aggregation and breakage at a given time of  
259 flocculation, and its average size tends to a stable value, *i.e.* a limiting size, for a given shear rate  
260 as the steady state regime is reached. When little variation is observed in floc size, the average  
261 size of  $d$  remains oscillating slightly around a maximum value, which is referred to as the plateau.

262 The plateau was determined from the incremental variation of the average diameter ( $d$ ) during  
263 flocculation. This variation tends to a narrow range because of the dynamic steady state. The  
264 incremental variation can be determined by:

$$265 \quad \Delta d_i = \left| \frac{(d_i - d_{i-1})}{d_i} \right| \quad (2)$$

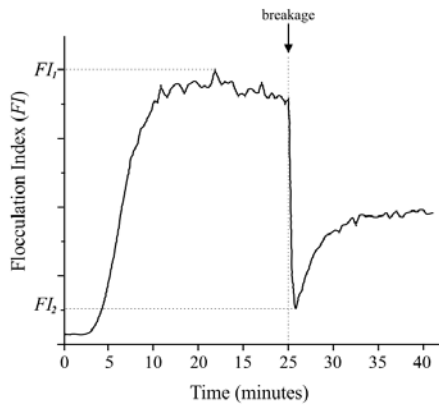
266 where  $\Delta d_i$  is the incremental variation of average diameter between the time interval  $t_i - t_{i-1}$ , with  $i$   
267 = 1, 2, ..., n.

268 The typical value of the diameter in the plateau was then determined from the average of  
269 diameters within  $\Delta d \leq 10\%$ . Hypothesis tests were also performed to confirm the plateau with  
270 significance of 0.05.

271 The analysis based on light scattering was done through the  $FI$  signal generated from the PDA.

272 The maximum value observed in the stationary flocculation phase was adopted once the plateau

273 was reached at that time interval. For  $FI_2$ , the value adopted was the minimum point at the instant  
 274 of the induced rupture, following Li *et al.* (2007). Here, the rupture shear rate of  $800 \text{ s}^{-1}$  was  
 275 applied for 10 seconds, at the flocculation time of 25 minutes. Figure 3 schematically shows how  
 276  $FI_1$  and  $FI_2$  are determined from the  $FI$  signal.



277

278 Figure 3. Schematic representation of the  $FI$  signal, with indication of the values of  $FI_1$ ,  $FI_2$  and  
 279 induced breakage by applying velocity gradient of  $800 \text{ s}^{-1}$  at 25 minutes (adapted from Li *et al.*,  
 280 2007).

281

## 282 2.6 Floc strength indicators

283 As mentioned in previous sections, the floc strength indicators presented here were determined  
 284 using both image analysis and PDA. For the image analysis method,  $d$  values were taken, whilst  
 285 for PDA only  $FI$  signals were used.

### 286 Floc strength coefficient ( $\gamma$ )

287 The floc strength coefficient ( $\gamma$ ) was obtained from image analysis using Equation 3 that  
 288 describes the stable size determined from image analysis as a function of the mean velocity  
 289 gradient applied to the system during flocculation, firstly suggested by Parker *et al.* (1972):

$$290 \quad d = C \cdot G^{-\gamma} \quad (3)$$

291 where  $C$  is the multiplicative constant ( $\mu\text{m/s}$ ),  $G$  is the average velocity gradient ( $\text{s}^{-1}$ ), and  $\gamma$  is  
 292 the floc strength coefficient (dimensionless), obtained from stable floc size.

293 The floc strength coefficient ( $\gamma$ ) can be calculated using mean, median and longest length of flocs  
 294 with nearly the same results, as reported by Leentvaar and Rebhun (1983). For the results

295 presented here,  $d$  values were calculated using the longest length of flocs obtained during  
296 flocculation from different shear rates according to Equation 1.

297 The  $\ln-\ln$  plot of Equation 3 against the average gradient velocity **applied during flocculation**  
298 results in a line, which its slope is indicative of floc strength. The inverse relationship of  
299 proportionality indicates that the higher the value of  $\gamma$ , the more prone the floc is to breakage  
300 under increasing shear rates, resulting in smaller aggregates (Li *et al.*, 2007). Therefore, the value  
301 of  $\gamma$  is considered as an indicator of its strength. This concept was proposed by Parker *et al.*  
302 (1972) and is adopted in the study of Li *et al.* (2007). Here, the floc strength coefficient ( $\gamma$ ) was  
303 determined from the slope of linear best fit to the  $\ln-\ln$  plot of Equation 3, using experimental  
304 data for the study waters. It is worth noting that the value of  $C$  can also be used as a floc strength  
305 indicator, but only within the same experimental conditions, as its value depends upon the  
306 method used for particle size measurements and the choice of the characteristic value of  $d$  (Jarvis  
307 *et al.*, 2005).

#### 308 *Strength factor (SF)*

309 The strength factor ( $SF$ ) has been previously used by several researchers (*e.g.* Li *et al.*, 2007; Yu  
310 *et al.*, 2010b and 2015; Su *et al.*, 2017) to compare the breakage and the strength of flocs in  
311 different shear rate conditions for Al-Kaolin aggregates. The results of these studies indicate that  
312 this parameter can be effectively used as a floc strength index.  $SF$  is calculated based on  $FI$   
313 signals only and used to characterize the aggregate size maintenance capacity, following  
314 Yukselen and Gregory (2002):

$$315 \quad SF (\%) = \frac{FI_2}{FI_1} 100 \quad (4)$$

316 where  $FI_1$  is the maximum  $FI$  value before breakage, and  $FI_2$  is the  $FI$  value right after the  
317 breakage period, as shown in Figure 3. In this study,  $FI_1$  was calculated from different shear rates  
318 and  $FI_2$  was always determined after applying a shear rate of  $800 \text{ s}^{-1}$ , as described in Section 2.5.

319 High values of the  $SF$  indicate that flocs are better able to withstand shear rates, and therefore, the  
320 higher the value of  $SF$ , the stronger the flocs can be considered for a given rupture shear rate  
321 (Jarvis *et al.*, 2005). It is important to note that  $SF$  is not constant, the shear rate applied during

322 the breakage strongly affects  $FI_2$  (Yu *et al.*, 2010b), and so,  $SF$  can only be compared for similar  
323 **induced** rupture conditions. Here, the average velocity gradient of  $800 \text{ s}^{-1}$  was applied for rupture.

324 *Hydrodynamic disturbance ( $\sigma$ )*

325 In addition to the above-mentioned empirical methods for obtaining a force coefficient, Bache *et*  
326 *al.* (1997) proposed a theoretical method where the mean force applied per unit area of the  
327 system,  $\sigma$  ( $\text{N/m}^2$ ), could be determined by:

$$328 \quad \sigma = \frac{4\sqrt{3}}{3} \frac{\rho_w \mathcal{E}^{3/4} d}{\nu^{1/4}} \quad (5)$$

329 where  $\rho_w$  is the density of the water ( $\text{kg/m}^3$ ),  $\mathcal{E}$  is the local energy dissipation rate per unit mass  
330 ( $\text{m}^2/\text{s}^3$ ),  $d$  is the average of the longest length of aggregates at a given time, measured by image  
331 analysis (m) and  $\nu$  is the kinematic viscosity ( $\text{m}^2/\text{s}$ ) at room temperature of  $20 \pm 2^\circ\text{C}$ .

332 Parameter  $\mathcal{E}$  is usually replaced by  $\bar{\mathcal{E}}$  (Equation 6), which is the average rate of dissipation of the  
333 local energy per unit mass and is directly proportional to  $G$ , a parameter easily administered  
334 during the experiment:

$$335 \quad \bar{\mathcal{E}} = \nu G^2 \quad (6)$$

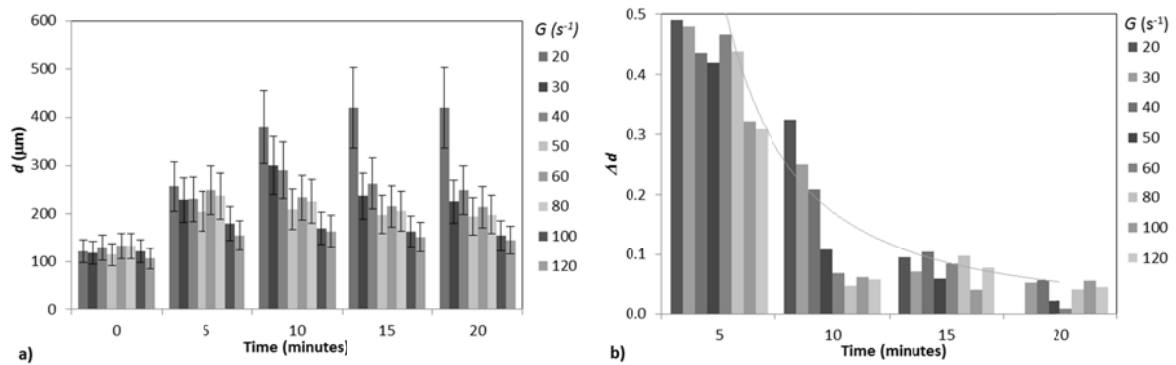
336 where  $\nu$  is the kinematic viscosity ( $\text{m}^2/\text{s}$ ).

### 337 **3. Results and Discussion**

#### 338 *3.1 Image analysis*

339 Figure 4, as an example, presents the time evolution of  $d$  and  $\Delta d$  obtained from Equations 1 and  
340 2, respectively, for various velocity gradients ( $G$ ) applied to study water type 2. For  $d$  evolution  
341 (Figure 4-a), aggregates have grown for time intervals between 5 and 10 minutes and for  $G$  from  
342 20 to  $40 \text{ s}^{-1}$ . After 10 minutes of flocculation, only  $G$  of  $20 \text{ s}^{-1}$  has resulted in aggregates  
343 increment for  $d$ . Consequently, the incremental variation of floc size (Figure 4-b) is observed to  
344 be smaller than 10% for the majority of the analysed velocity gradients during the flocculation at  
345 times 10-15 and 15- 20 minutes (except for  $G$  of 20, 30 and  $40 \text{ s}^{-1}$ ), indicating the establishment  
346 of steady-state conditions. Thus,  $d$  was obtained by averaging  $d$  during the period 15-20 minutes,  
347 when significant stability was observed, *i.e.* when the stable size of  $d$  was reached. For these time  
348 intervals, test of hypothesis has shown that there is no significant difference between the two

351 water types for p-value of 0.05, *i.e.* for both Al-Humic and Al-Kaolin the average diameter did  
 352 not change for time intervals from 15 to 20 minutes, making it possible to confirm the plateau.



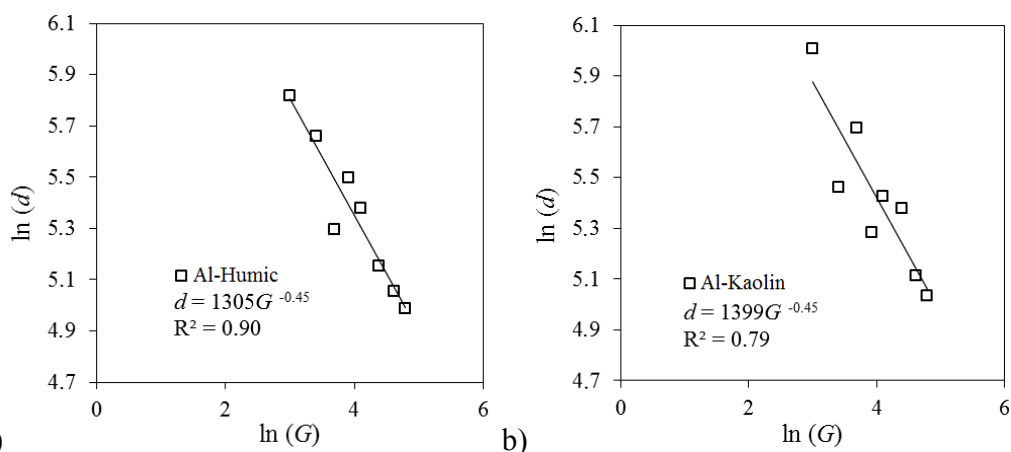
357 a) b)  
 358 Figure 4. Time evolution of (a)  $d$  and (b)  $\Delta d$  during flocculation time (for discrete intervals of 5,  
 359 10, 15 and 20 minutes) for water type 2. Fluctuation bars in (a), represent standard derivations  
 360 and the decay curve in (b), represents the overall trend of  $\Delta d$  during time. Time zero in Fig. 4-a  
 361 shows flocs size measurements in the very beginning of flocculation and those results were used  
 362 as  $d_{i-1}$  for  $\Delta d$  calculation in time of 5 minutes, as Equation 2.

365 Figure 5 shows the relationship between  $\ln(d)$ , calculated by Equation 1, and  $\ln(G)$ , where the  
 366 slope of the trend line, as described by Equation 3, indicates the floc strength coefficient  $\gamma$ . Once  
 367  $\gamma$  value remains constant, any variant characteristic of  $d$  (*i.e.* mean, median or maximum length)  
 368 can be used for comparing results among different studies (Jarvis *et al.*, 2005). A decreasing  
 369 tendency of the stable size  $d$  in response to the increase of  $G$  was observed at a rate near 0.45 for  
 370 the two study waters, which is in the range of 0.44 to 0.63 reported by other researchers (*e.g.*  
 371 Bache and Rasool, 2001; Francois, 1987; Li *et al.*, 2007) when using alum as coagulant for Al-  
 372 Humic and Al-Kaolin flocs.

373 The obtained  $\gamma$  value for the two study waters indicates that Al-Humic and Al-Kaolin flocs are  
 374 similarly able to resist shear rates, as the steepness of the  $\ln-\ln$  plot slopes are nearly the same for  
 375 both waters (0.45). The analysis of  $C$  from Equation 3 is not commonly used for floc strength  
 376 evaluation, as it depends upon which characteristic of  $d$  has been used, and wide variation  
 377 between different studies has been reported, *e.g.* from  $\ln C$  of 7.1 to 9.4 according to Bache *et al.*  
 378 (1999) and Bache and Rasool (2001), respectively. However,  $C$  can be also used to compare floc  
 379 strength within specific experimental system (Jarvis *et al.*, 2005). Results presented here have  
 380 shown  $C$  values of 1305 ( $\ln C$  of 7.17) and of 1399 ( $\ln C$  of 7.24) for Al-Humic and Al-Kaolin,

373 respectively, thus reinforcing that Al-Humic and Al-Kaolin have nearly the same ability to resist  
 374 applied shear forces. These results are in agreement with the finding by Yu *et al.* (2015) who  
 375 found that the nature of primary particles has no influence on floc strength when sweep  
 376 coagulation mechanism is applied and once flocs rapidly grow and incorporate most particles  
 377 within the hydroxide precipitate. Also, the use of a non-intrusive technique, such as the image  
 378 analysis system here applied, permits to confirm the previous findings by Yu *et al.* (2015), once it  
 379 is not influenced by possible interferences caused by samples extraction and light scattering, as  
 380 presented by Gregory (2009) and Yu *et al.* (2015).

381 The analysis of strength coefficient ( $\gamma$ ) can also be related to turbulent shear patterns due to eddy  
 382 size, as proposed by Biggs and Lant (2000) and Bache (2004), resulting in different floc breakage  
 383 modes during flocculation. Based on the analysis of the dominant mode of floc degradation  
 384 presented by Parker (1972) and François (1987), the results presented here for  $\gamma$  (Figure 5)  
 385 indicate that the flocs are more prone to breakage due to a dominant effect of fragmentation, as  
 386 the result of the viscous energy dissipation, once the floc strength coefficient  $\gamma$  was around the  
 387 theoretical value of 0.5. This is an indication that small eddies (*i.e.* the turbulence micro-scale) is  
 388 of a similar order of magnitude to the flocs sizes (Mühle, 1993; Jarvis *et al.*, 2005). However,  
 389 fragmentation and erosion are expected to occur at the same time, as large flocs in an aggregated  
 390 system may be larger than the micro-scale whilst smaller flocs may be smaller than micro-scale  
 391 (Biggs and Lant, 2000).



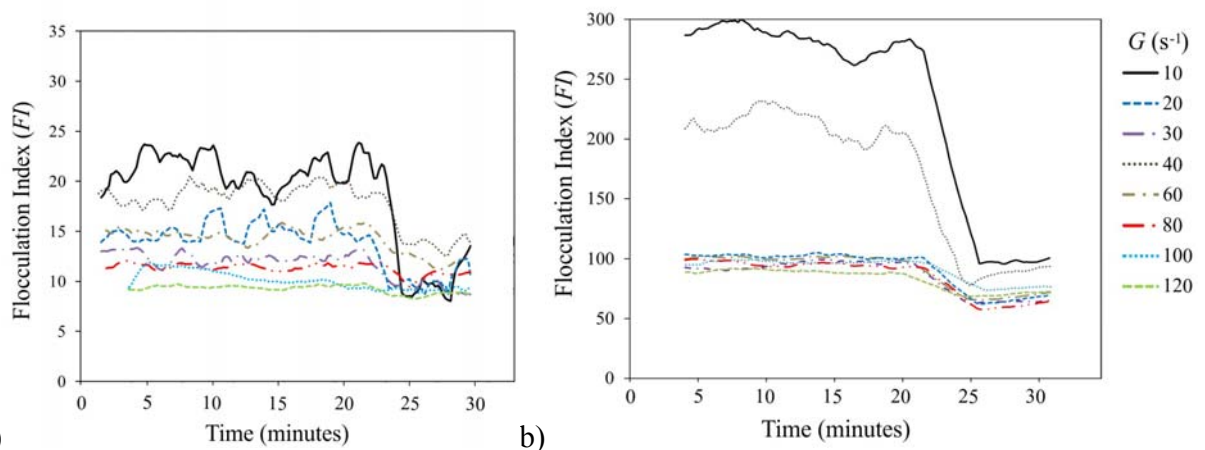
392 a) 393 Figure 5. Relationship between  $\ln d$  versus  $\ln G$  during flocculation: (a) water type 1 – Al-Humic  
 394 and (b) water type 2 – Al-Kaolin.  $\ln d$  was obtained by averaging  $d$  during the period 15-20  
 395 minutes, where  $\Delta d < 10\%$  was observed.



396 3.2 Light scattering

397 Figure 6 shows the temporal evolution of the  $FI$  signal (obtained by PDA) in the tests carried out.  
398 It is clearly observed that in the flocculation [0-20 minutes] and regrowth [25-40 minutes] phases,  
399 the floc size tend towards a stabilized plateau. The sharp drop of  $FI$  at 25 minutes was the point  
400 where the induced breakage occurred. The difference in the signal scale between the two study  
401 waters is caused by the different light scattering properties, *e.g.* floc density and scattering cross-  
402 section, which are also dependent on both particle concentration (in terms of volume, mostly) and  
403 type (Gregory, 2009). This difference has important implications for the monitoring of floc size  
404 by light scattering methods as also observed by Yu *et al.* (2015). Similar fluctuation on  $FI$  values  
405 were observed by Gregory (2009), while studying optical proprieties of flocs using PDA for  
406 different waters. The author concluded that scattering cross-section is expected to be different  
407 when different concentration of impurities, as clay, are within flocs and so  $FI$  signals vary.  
408 However, the results obtained by Gregory (2009) have shown that curves are rather similar in  
409 shape, showing the same relative increase in  $FI$  during floc formation. Therefore, although  
410 scattering proprieties can limit direct comparisons of  $FI$  values among different waters, it is not  
411 expected to affect the strength factor ( $SF$ ) given by Equation 4, once it is determined as a ratio for  
412 the same water, *i.e.* subjected to the same scattering properties.

413



414 a) 415 Figure 6. Time evolution of FI for different velocity gradients,  $G$  before and after induced  
416 breakage using  $800 s^{-1}$  at time 25 minutes. (a) water type 1 for Al-Humic acid and (b) water type  
417 2 for Al-Kaolin.

418

419 *3.3 Combined analyses of image and photometric dispersion methods*

420 Both analyses of image and photometric dispersion methods permitted to compare and correlate  
421 data obtained from two different techniques *i.e.* intrusive and non-intrusive methods. Tables 1  
422 and 2 present a comparison between the stable size and the floc strength for eight different  
423 velocity gradients ( $G$ ). The floc strength indicators presented are local stress ( $\sigma$ ) and the force  
424 factor ( $SF$ ).

425 It is observed that, for each of the studied waters,  $SF$ ,  $\sigma$  and  $d$  were strongly correlated with the  
426 parameter  $G$ , resulting in Pearson correlation coefficient of 0.95, 0.99 and -0.89 for Al-Humic  
427 and of 0.90, 0.99 and -0.80 for Al-Kaolin, respectively. Results found here corroborate well with  
428 Li *et al.* (2007), who found that flocs formed at higher shear intensities have a small size and are  
429 more resistant to breakage than those formed from lower ones. Floc resistance is determined by  
430 both hydraulic shear rates and the strength of flocs bonds, which withstand shear forces during  
431 floc formation (Jarvis *et al.*, 2005; Gregory, 2009). During floc formation in high shear rates, the  
432 weak bonds might be broken, promoting a kind of selection, which results in floc fragments with  
433 strong bonds. Therefore, with the higher shear rates, only the strongest bonds, which are more  
434 likely to resist to the abrupt  $G$  variations, are maintained (Li *et al.*, 2007). This fact was shown by  
435 the increase in  $SF$  value from 29.7% for  $G$  of  $20 \text{ s}^{-1}$  to 78.6% for  $G$  of  $120 \text{ s}^{-1}$  in water type 1 and  
436 33.3% for  $G$  of  $20 \text{ s}^{-1}$  to 85.2% for  $G$  of  $120 \text{ s}^{-1}$  in water type 2.

437 Results in Tables 1 and 2 also suggested that the effect of  $G$  on  $SF$  might be more relevant for  $G$   
438 from 20 to  $40 \text{ s}^{-1}$ , and that  $d$  values can also decrease dramatically with the increase of  $G$ ,  
439 indicating there might be a limit above which floc strength is slightly affected by shear rate, but it  
440 can strongly affect floc formation.

441 Results obtained from the two other strength indices used here seem to agree with the strength  
442 coefficient ( $\gamma$ ) analysis. The values of  $\sigma$  were nearly the same for water types 1 and 2, ranging  
443 from 0.08 to 0.47 and from 0.07 to 0.44, respectively, with Pearson correlation coefficient ( $r$ )  
444 between waters near to 1 ( $r = 0.97$ ). These results are in agreement with previous work done by  
445 Bache *et al.* (1999) who found Al-Humic flocs strength in the range of 0.08 to  $0.42 \text{ N/m}^2$ , and  
446 close to the study by Li *et al.* (2007), who found Al-Kaolin flocs strength in the range of 0.01 to

447 0.24 N/m<sup>2</sup>. Moreover, ANOVA test for  $\sigma$  variation with  $G$  indicates that floc strength is not  
 448 different between Al-Humic and Al-Kaolin for 0.05 of significance (p-value over 0.05), but it  
 449 depends on  $G$  and  $d$  only.

450 Regarding the strength factor ( $SF$ ), results also have shown slight differences between aggregates  
 451 formed from Al-Humic and Al-Kaolin. Again, the ANOVA test for  $SF$  with  $G$  indicates that floc  
 452 strength is not different between Al-Humic and Al-Kaolin for 0.05 of significance, but it depends  
 453 on  $G$  and  $d$  only.

454 Despite the fact that the intrinsic characteristics of flocs formed from Al-Kaolin and Al-Humic,  
 455 namely, the scattering cross-section, altered  $FI$  measurements it seems that it did not affect floc  
 456 strength measurements by  $SF$ , as it is in agreement with the other two strength indicators.  
 457 Therefore, it is not expected that optical proprieties affect physical proprieties measurements,  
 458 such as resistance, and so the  $FI$  signal has been used by many researchers as an aggregation  
 459 indicator and as well as an indirect measurement of floc strength, *e.g.* Li *et al.* (2007), Yu *et al.*  
 460 (2010b and 2011), Su *et al.* (2017).

461

$G$	$SF$	$\sigma$	$d$
(s <sup>-1</sup> )	(%)	N/m <sup>2</sup>	μm
20	36.73	0.07	337
30	56.82	0.11	287
40	55.56	0.12	200
50	69.70	0.20	245
60	69.34	0.23	217
80	83.33	0.29	173
100	83.33	0.36	157
120	95.00	0.44	146

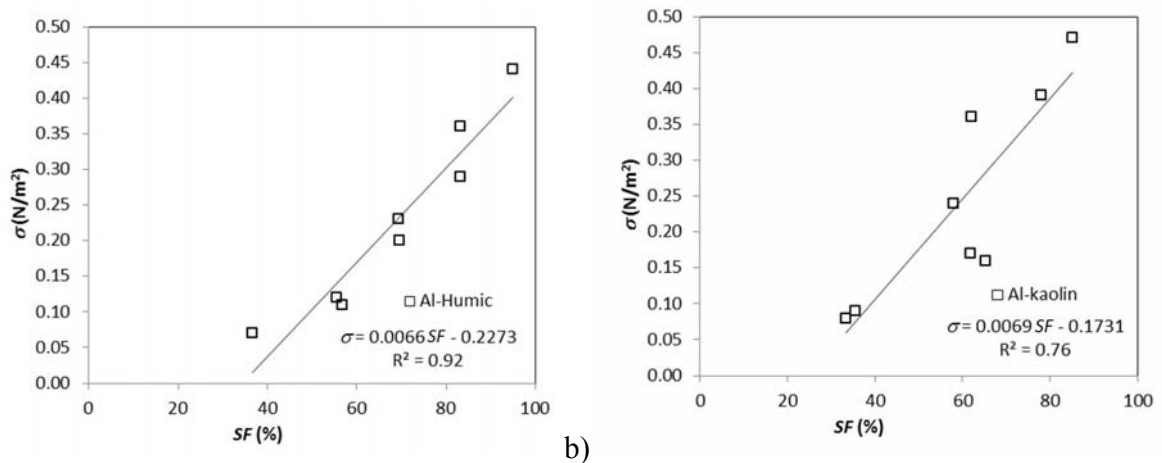
Table 1. Shear rates ( $G$ ), strength indexes ( $SF$  and  $\sigma$ ) and stable size ( $d$ ) for water type 1 (Al-Humic acid) during flocculation.

$G$	$SF$	$\sigma$	$d$
(s <sup>-1</sup> )	(%)	N/m <sup>2</sup>	μm
20	33.33	0.08	407
30	35.56	0.09	236
40	61.82	0.17	298
50	65.42	0.16	197
60	58.00	0.24	228
80	62.00	0.36	217
100	78.00	0.39	167
120	85.23	0.47	154

Table 2. Shear rates ( $G$ ), strength indexes ( $SF$  and  $\sigma$ ) and stable size ( $d$ ) for water type 2 (Al-Kaolin) during flocculation.

462 Figure 7 shows the relationship of the strength factor ( $SF$ ), obtained from PDA, with the  
 463 parameter  $\sigma$ , which was calculated from image analysis data. It is observed that for both water

464 types, relatively high regression coefficients are obtained between  $SF$  and  $\sigma$  ( $R^2$  of 0.92 and 0.76  
 465 for Al-Humic and Al-Kaolin, respectively) and a similar slope (close to 0.0070) is found for  
 466  $\sigma/SF$ . It is apparent that the values of both mentioned parameters enhance with increase in  $G$ ,  
 467 which are in agreement with results presented by Li *et al.* (2007) and Jarvis *et al.* (2005). Further,  
 468 Pearson correlation coefficient between  $SF$  and  $\sigma$  resulted in 0.96 and in 0.87 for Al-Humic and  
 469 Al-Kaolin, respectively. **These strong correlations have confirmed that the macroscopic approach**  
 470 **represented by  $SF$  is consistent with the theoretical method for different types of water, despite of**  
 471 **the different methods used and the variations of  $FI$  signals.**



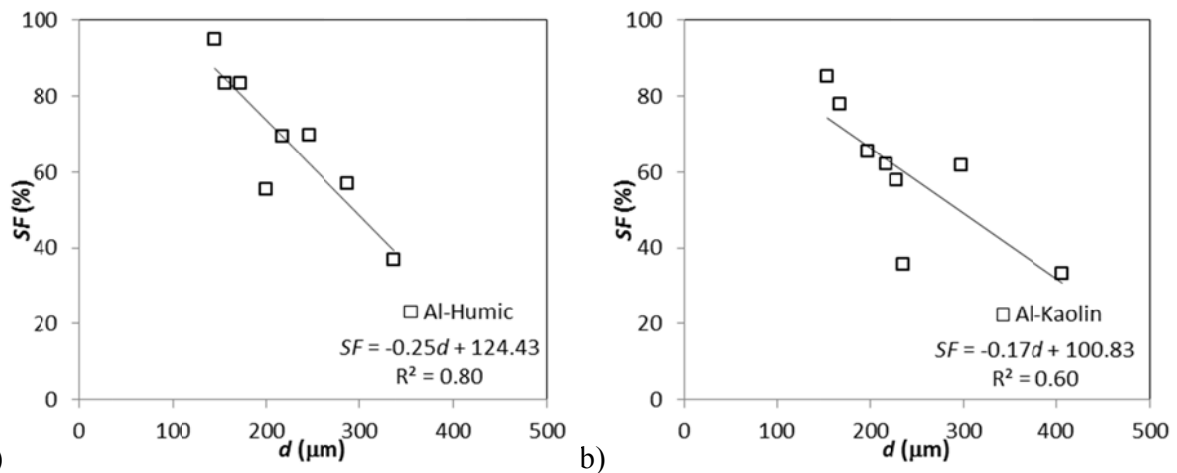
472 a) b)  
 473 Figure 7. Relationship between  $SF$  and  $\sigma$  for (a) water type 1 for Al-Humic acid and (b) water  
 474 type 2 for Al-Kaolin.

475 Figure 8 shows the relationship between  $SF$  and  $d$ , *i.e.* the specific relationship between the  
 476 strength force indicator obtained from PDA and values of average floc length, monitored by  
 477 image analysis. The strength factor ( $SF$ ) behaved nearly the same as  $d$  varied for Al-Humic and  
 478 Al-Kaolin flocs, with smaller flocs resulting in higher resistant to  $G$  variations. These results are  
 479 in agreement with the other strength indicator reported here (Table 1 and 2).

480 Moreover, despite of the differences between the two methods (PDA and image analysis), results  
 481 indicate that the parameter  $d$ , derived from the non-intrusive image analysis, and  $SF$ , obtained  
 482 from the  $PDA$  signal, behaved in similar way, with  $R^2$  values near to 0.80 for Al-Humic and 0.60  
 483 for Al-Kaolin.

484 The lower  $R^2$  value for Al-Kaolin is believed to be attributed to the different scattering area, as  
 485 previously discussed. However, this does not explain why  $SF$  for Al-Humic and Al-Kaolin

493 behaved with no significant difference (p-value over 0.05), when exposed to rupture shear rate of  
 494  $800 \text{ s}^{-1}$ . A possible explanation is that flocs formed from sweep coagulation mechanism are  
 495 bigger than those formed from charge neutralization and their physical properties are likely  
 496 determined by coagulant only, as pointed out by Yu *et al.* (2015). Besides, floc characteristic size  
 497 was calculated based on the average of longest length, and so, it is expected that large flocs are  
 498 more prone to breakage by fragmentation when exposed to micro-scale dissipating eddies, thus  
 499 resulting in similar strength for Al-Humic and Al-Kaolin aggregates.



494 a) Figure 8. Relationship between  $SF$  and  $d$ : (a) water type 1 – Al-Humic and (b) water type 2 – Al-  
 496 Kaolin.  
 497

#### 497 4. Conclusions

405 Floc size and strength play an important role in separation processes used in water and  
 406 wastewater treatment, and the influence of different primary particles on the floc strength is still  
 407 poorly understood. The evidence that aggregates resistance is invariable with particles when  
 408 sweep coagulation is applied needs to be further investigated. Here, two aggregates formed by  
 409 Al-Humic and Al-Kaolin during flocculation were investigated using two techniques, namely  
 410 intrusive photometric dispersion analyser and non-intrusive image system. Both techniques were  
 411 applied to determine three floc strength indexes: the strength factors ( $SF$ ), the local stress ( $\sigma$ ) and  
 412 floc strength coefficient ( $\gamma$ ). The main conclusions of this work are:

506

- 508 1. For Al-Humic and Al-Kaolin flocs, the strength factors ( $SF$ ) and the local stress ( $\sigma$ ) have  
 509 a positive variation in response to the increase of  $G$  because the high shear forces select

508 the strongest bonds within the aggregates. This means that higher  $G$  produces more  
509 resistant aggregates, however the size dependence for an individual separation process  
510 efficiency must be considered.

511 2. The comparison between the aggregates strength for Al-Humic acid and Al-Kaolin using  
512 floc strength coefficient ( $\gamma$ ) indicates that both aggregates have nearly the same resistance,  
513 possible due to the precipitate hydroxide of alum mostly influencing floc size and  
514 strength. This finding reinforces the perspective that particles within a floc may have  
515 slight, or even no influence, on the floc strength when sweep coagulation is applied.

516 3. The intrusive photometric dispersion analyser and non-intrusive image-based system used  
517 in this study produced well correlated parameters, with a similar behaviour. However, the  
518 non-intrusive image method proved to be more reliable, as images are not influenced by  
519 the optical characteristics of the flocs.

## 520 **Acknowledgements**

521 Rodrigo B. Moruzzi is grateful to São Paulo Research Foundation (*Fundação de Amparo à*  
522 *Pesquisa do Estado de São Paulo*—FAPESP) Proc. 2017/19195-7 for financial support.

## 523 **References**

- 524 1. Bache, D.H. Floc rupture and turbulence: a framework for analysis. *Chem. Eng. Sci.* 59,  
525 2521–2534. (2004). doi: <http://dx.doi.org/10.1016%2Fj.ces.2004.01.055>
- 526 2. Bache, D.H., Al-Ani, S.H. Development of a system for evaluating floc strength. *Water*  
527 *Sci. Technol.* 21, 529–537. (1989). doi: <https://doi.org/10.2166/wst.1989.0255>
- 528 3. Bache, D.H., Johnson, C., McGilligan, J.F., Rasool, E. A conceptual view of floc structure  
529 in the sweep floc domain. *Water Sci. Technol.* 36 (4), 49–56. (1997). doi:  
530 [https://doi.org/10.1016/S0273-1223\(97\)00418-6](https://doi.org/10.1016/S0273-1223(97)00418-6)
- 531 4. Bache, D.H., Rasool, E., Moffatt, D., McGilligan, F.J. On the strength and character of  
532 alumino-humic flocs. *Water Sci. Technol.* 40 (9), 81–88. (1999). doi:  
533 [https://doi.org/10.1016/S0273-1223\(99\)00643-5](https://doi.org/10.1016/S0273-1223(99)00643-5)
- 534 5. Bache, D.H., Rasool, E.R. Characteristics of alumina humic flocs in relation to DAF  
535 performance. *Water Sci. Technol.* 43 (8), 203–208. (2001). doi:  
536 <https://doi.org/10.2166/wst.2001.0495>

- 537 6. Biggs, C.A., Lant, P.A. Activated sludge flocculation: on-line determination of floc size  
538 and the effect of shear. *Water Res.* 34, 2542–2550. (2000).
- 539 7. Chakraborti, R. K.; Gardner, K. H.; Atkinson, J. F.; Van Benschoten, J. E. Changes in  
540 fractal dimension during aggregation. *Water Research.* v.37. p. 873–883. (2003).
- 541 8. Francois, R.J. Strength of aluminium hydroxide flocs. *Water Res.* 21, 1023–1030 (1987).  
542 doi: [https://doi.org/10.1016/0043-1354\(87\)90023-6](https://doi.org/10.1016/0043-1354(87)90023-6)
- 543 9. Gregory and D.W. Nelson, A new optical method for flocculation monitoring. In *Solid-  
544 Liquid Separation* (J. Gregory, Ed.) Ellis Horwood, Chichester, pp 172-182. (1984).
- 545 10. Gregory, J. Monitoring particle aggregation process. *Advances in Colloids and Interfaces*  
546 v.147-148, 109-123. (2009). doi: <https://doi.org/10.1016/j.cis.2008.09.003>
- 547 11. Gregory, J. Optical monitoring of particle aggregates. *J. Environ. Sci.* 21, 2e7. (2009).  
548 doi: [https://doi.org/10.1016/S1001-0742\(09\)60002-4](https://doi.org/10.1016/S1001-0742(09)60002-4)
- 549 12. Gregory, J., Monitoring floc formation and breakage. In: *Proceedings of the Nano and  
550 Micro Particles in Water and Wastewater Treatment Conference.* International Water  
551 Association, Zurich September (2003)
- 552 13. Gregory, J., Nelson, D.W. Monitoring of aggregates in flowing suspension. *Colloids Surf.*  
553 18, 175–188, (1986).
- 554 14. Jarvis P., Jefferson B., Gregory, J. and Parsons, S. A. A review of floc strength and  
555 breakage. *Water Res.* 39, 3121-3137. (2005). doi:  
556 <http://dx.doi.org/10.1016/j.watres.2005.05.022>
- 557 15. Li, T. Zhu, Z., Wang, D., Yao, C. and Tang, H. The strength and fractal dimension  
558 characteristics of alum–kaolin flocs. *International Journal Of Mineral Processing*,  
559 Beijing, Pr China, v. 82, n. 1, 23-29. (2007). doi: [https://doi.org/10.1016/S0273-  
560 1223\(99\)00643-5](https://doi.org/10.1016/S0273-1223(99)00643-5)
- 561 16. Leentvaar, J., Rebhun, M. Strength of ferric hydroxide flocs. *Water Res.* 17, 895–902.  
562 (1983).
- 563 17. Mikkelsen, L.H., Keiding, K. The shear sensitivity of activated sludge: an evaluation of  
564 the possibility for a standardised floc strength test. *Water Res.* 36, 2931–2940. (2002).  
565 doi: [https://doi.org/10.1016/S0043-1354\(01\)00518-8](https://doi.org/10.1016/S0043-1354(01)00518-8)
- 566 18. Mühle, K. Floc stability in laminar and turbulent flow. In: Dobias, B. (Ed.), *Coagulation  
567 and Flocculation.* Dekker, New York, pp. 355–390. (1993).

- 568 19. Oliveira, A.L. de, Moreno, P., Silva, P.A.G. da, Julio, M.D. and Moruzzi, R.B. Effects of  
569 the fractal structure and size distribution of flocs on the removal of particulate matter.  
570 *Desalination and Water Treatment.*, Vol. 57 (36). 1-12. (2015). doi:  
571 <https://doi.org/10.1080/19443994.2015.1081833>
- 572 20. Parker, D.S., Kaufman, W.J., Jenkins, D. Floc breakup in turbulent flocculation processes.  
573 *J. Sanit. Eng. Div.: Proc. Am. Soc. Civ. Eng. SA1*, 79–99. (1972). doi:  
574 <https://pubs.acs.org/doi/abs/10.1021/la980763o>
- 575 21. Moruzzi, R. B., Silva, P. A. G. Reversibility of Al-Kaolin and Al-Humic aggregates  
576 monitored by stable diameter and size distribution. *Brazilian Journal of Chemical*  
577 *Engineering.*, Vol. 35 (3). 1029-1038. (2018). doi: [dx.doi.org/10.1590/0104-](dx.doi.org/10.1590/0104-6632.20180353s20170098)  
578 [6632.20180353s20170098](dx.doi.org/10.1590/0104-6632.20180353s20170098)
- 579 22. Zhaoyang Su, Xing Li, Yanling Yang. Regrowth ability and coagulation behavior by  
580 second dose: Breakage during the initial flocculation phase. *Colloids and Surfaces A* 527,  
581 109–114. (2017). doi: <http://dx.doi.org/10.1016/j.colsurfa.2017.05.034>
- 582 23. Wang, Y., Gao, B., Xu, X., Xua, W., Xub, G. Characterization of floc size, strength and  
583 structure in various aluminum coagulants treatment. *Journal of Colloid and Interface*  
584 *Science* v332, 354–359. (2009). doi: <https://doi.org/10.1016/j.jcis.2009.01.002>
- 585 24. Watanabe, Y., Flocculation and me. *Water Research.* (2017). doi:  
586 <https://doi.org/10.1016/j.watres.2016.12.035>
- 587 25. Yu, W., Gregory, J. and Campos, L. The effect of additional coagulant on the re-growth  
588 of alum–kaolin flocs. *Separation and Purification Technology* v74, 305–309. (2010a). doi:  
589 <https://doi.org/10.1016/j.seppur.2010.06.020>
- 590 26. Younker, J. M., Walsh, M. E. Effect of adsorbent addition on floc formation and  
591 clarification. *Water Research* 98. (2016). doi:  
592 <https://doi.org/10.1016/j.watres.2016.03.044>
- 593 27. Yu, W., Gregory, J. and Campos, L., Breakage and Regrowth of al Humic Flocs – Effect  
594 of additional Coagulant Dosage. *Environ. Sci. Technol*, no. 44. (2010b). doi:  
595 <http://dx.doi.org/10.1021/es1007627>
- 596 28. Yu, W., Gregory, J., Campos, L., Breakage and re-growth of flocs: Effect of additional  
597 doses of coagulant species. *Water Research*, 45. (2011). doi:  
598 <https://doi.org/10.1016/j.watres.2011.10.016>



- 599 29. Yu, W., Gregory, J., Campos, L., Graham, N. Dependence of floc properties on coagulant  
600 type, dosing mode and nature of particles. *Water Research* 68, p 119-126. (2015). doi:  
601 <https://doi.org/10.1016/j.watres.2014.09.045>
- 602 30. Yu, W., Hu, C., Liu, H., Qu, J. Effect of dosage strategy on Al-humic flocs growth and re-  
603 growth. *Colloids and Surfaces A: Physicochem. Eng. Aspects*, 404, 106–111. (2012). doi:  
604 <https://doi.org/10.1016/j.colsurfa.2012.04.033>
- 605 31. Yukselen, M. A. and Gregory, J. The reversibility of flocs breakage. *International Journal*  
606 *of Mineral Processing*, v. 73, no. 2-4, p. 251-259. (2004). doi:  
607 [https://doi.org/10.1016/S0301-7516\(03\)00077-2](https://doi.org/10.1016/S0301-7516(03)00077-2)
- 608 32. Yukselen, M.A. and Gregory, J. Breakage and reformation of alum flocs. *Environ. Eng.*  
609 *Sci.* no. 19, p. 229–236. (2002). doi: <https://doi.org/10.1089/109287502760271544>
- 610 33. Zhong, R., Zhang, X., Xiao F., Li, X., Cai Z., Effects of humic acid on physical and  
611 hydrodynamic properties of kaolin flocs by particle image velocimetry. *Water Research*  
612 45. (2011). doi: <https://doi.org/10.1016/j.watres.2011.05.006>